QUANTIFICATION OF THE EFFECTS OF THE INLET WAVEFORM ON HEMODYNAMICS INSIDE INTERNAL CAROTID ARTERIES USING COMPUTATIONAL FLUID DYNAMICS.

Djalal SEKHANE, Karim MANSOUR

Laboratory of Electronic Materials Studies for Medical Applications – Brothers Mentouri University – Constantine 1, Algeria.

Abstract

Hemodynamics is an important bio-mechanic factor, which is implicated in the regulation and regeneration function inside the vessels. However, disturbing in its factors may cause development of many vascular diseases. Computational fluid dynamics (CFD) is alternative tool, which is used to assess hemodynamic factors inside complex cerebral vessels.

The purpose of this study is to assess the influence of the inlet waveforms under the same mean inflow on different hemodynamic factors inside Internal Carotid Arteries (ICA), using computational fluid dynamics combined to patient specific MRI images.

Four numerical models of (ICA) were reconstructed from 3D TOF MRI images. Navies-Stokes equations were solved inside the geometry using finite elements method. Sixteen simulations using four-inlet waveforms and four ICA arteries were performed to quantify the influence of the inlet waveform on blood flow inside ICA.

Varying the Inlet waveform boundary conditions has important effects on the overall instantaneous hemodynamic factors assessed on the geometries. However, time averaged factor assessed has been constant for individual cases.

Information about patient-specific inlet waveform is necessary for the accuracy of the patient-specific computation.

Keywords: *ICA, CFD, inlet waveform, wall shear stress, pressure.*

Résumé

L'hémodynamique est un facteur biomécanique important qui est impliqué dans les fonctions de régulation et de régénération à l'intérieur des vaisseaux. Cependant, un déséquilibre des paramètres hémodynamique à l'intérieur des vaisseaux peut causer un développement de pathologies artérielles. La dynamique computationnelle des fluides (Computational Fluid Dynamics : CFD) est un outil qui peut être combiné à des images spécifiques de patients. Cette méthode permet d'évaluer les différents facteurs hémodynamiques à l'intérieur de géométries complexes.

L'objectif: dans ce travail est d'étudier l'effet de la forme d'onde d'entrée sur les facteurs hémodynamiques à l'intérieur des artères carotides intérieures (ICA) en utilisant la dynamique computationnelle des fluides combinée à des images spécifiques aux patients.

Quatre modèles numériques de l'ICA ont été reconstruits à partir des images IRM 3D TOF. Les équations de Navies Stokes ont été résolues en utilisant la méthode des éléments finis à l'intérieur des modèles numériques d'ICA. Seize simulations en utilisant quatre formes d'ondes ont été effectuées afin de quantifier l'influence de la forme d'onde d'entrée sur le flux sanguin à l'intérieur des ICA.

En utilisant différentes ondes d'entrée dans les modèles CFD, la forme d'onde d'entrée semble avoir une influence sur les différents facteurs hémodynamiques instantanés. Cependant, les moyennes temporelles de ces facteurs ne sont pas influencées.

Les données spécifiques du patient en utilisant le CFD combiné à des images spécifiques de celui-ci sont essentielles à l'évaluation du risque de développement de maladies cardiovasculaires.

Mots clés: *ICA, CFD, Forme d'onde d'entrée, Forces de cisaillement. Pression.*

ملخص

الاموديناميك هو عامل بيوميكانيكي هام مساعد على خصائص توازن و التجديد الخلايا داخل الاوعية الدموية. فقدان التوازن الاموديناميكي يمكن ان يكون سبب في تكون بعض امراض فيها. ميكانيك السوائل الحاسوبي هي أداة تمكن من دراسة الخصائص الاموديناميكية داخل الاوعية الدموية.

الهدف من هذا العمل هو دراسة تأثير شكل موجة الدخول على مختلف الخصائص الاموديناميكية باستعمال ميكانيك السوائل الحاسوبي وصور خاصة بالمرضى.

أربعة شرايين دماغية داخليةICA كونت من صور للرنين المغناطيسي من نوع MRI 3D TOF. ستة عشرة محاكات باستعمال أربع موجات دخول استعملت من اجل دراسة تأثير شكل موجة الدخول على مختلف الخصائص الاموديناميكية داخل كل شريان.

شكل موجة الدخول لها تأثير كبير على المعاملات الوقتية داخل الشرايين المدروسة في حين انه المعاملات بمعدل الوقت لم تتأثر.

معلومات شكل موجة الخاصة بكل مريض هامة من اجل دراسة إمكانية تكون بعض الامراض في الاوعية الدموية.

الكلمات المفتاحية: الشريان الدماغي الداخلي، ميكانيك السوائل الحاسوبي، شكل موجة الدخول، إجهاض القص، الضغط.

1. INTRODUCTION

Development of cerebrovascular diseases is a complex process in which several biomechanical and biological elements are involved. Hemodynamic, defined as the physical parts that govern blood flow [1], is an important biomechanical factor which prove its implication in genesis and the development of many arterial diseases [2, 3]. Therefore, understanding hemodynamic inside cerebral arteries is important to get an initial apprehending of the development of cerebrovascular diseases.

The cerebral vessels are composed by three layers: (i) tunica intima, (ii) tunica media, and (iii) tunica adventitia. Composed by a single layer of endothelial cells (ECs) [4], the tunica intima is the interface between the blood and the other tissues and organs, in where hemodynamic environment is a regulating factor of its structure [5].

Flowing blood applies two essential forces, Wall Shear Stress (WSS) and pressure. WSS is the parallel acting force to the wall, it can influence on the direction of ECs. Also, WSS has a crucial in the proliferation of ECs, which aids to repair the endothelium in the case of a toxic injury or mechanical desquamation. Moreover, it's implicated in the regulation of vascular tone by stimulating the production of nitric oxide (NO) which influence on the smooth muscle cells of the tunica media [6]. In addition to WSS forces, the pressure (P) which is the normal acting force to the wall, can also affect the physiology of the endothelium and the tension of the smooth muscle cells [7].

In the history of Intracranial Aneurysms (IA), the genesis is closely associated to disturbed hemodynamic flow conditions [8]. High WSS values can be a cause of the IA development. If WSS values is very high, it can cause a fragmentation of the ECs, which leads to an endothelium damage, while the low WSS affects the growth and the rupture of IA [9].

Computational fluid dynamics (CFD) is a powerful tool that can be combined with patient specific images, and which makes possible assessing hemodynamics inside realistic vessels [10]. This method is an alternative tool that can predict and provide safe information of flow factors [11, 12].

CFD model is composed by : (a) a geometry of the anatomical arterial form (b) a descriptive model of blood flow behaviour, and (c) the inflow and outflow boundaries conditions [12, 13]. The accuracy of the results of the CFD simulation depends on the precision of these components [2, 14].

Image-based patient specific CFD has been widely utilised to investigate the role of hemodynamic in the development of cerebrovascular diseases [10, 15-19] in where several boundaries conditions and parameters were investigated. In a previous work, we investigated the effects of changing heart rate on hemodynamic inside a healthy circle of Willis, and we found no quantitative effects on hemodynamic factors investigated [17]. In this paper, we present a study of the effect of change of inlet waveform in hemodynamics

inside Internal Carotid Arteries (ICA). The effect of changes of inlet waveform was assessed on WSS, pressure, Time Averaged Wall Shear Stress (TAWSS), and velocity streamlines.

2. MATERIAL AND METHODS:

A. Vascular model

In CFD, the geometric numeric model of the vessel is very important; its accuracy can highly affect the results of simulations [12]. The geometrical models used in CFD can be reconstructed from several imaging modalities [20]. However, the models must be reconstructed and truncated carefully because geometry characteristics can be influenced the hemodynamic factors [10].

To obtain the geometrical model of ICA, we performed a Time Of Flight (TOF) Magnetic Resonance Angiography (MRA) sequence for four patients with an 8-head array coil using GE HDxt system (General Electric Healthcare). To obtain a number varying from 178 to 215 slices (reconstruction matrix 512*512 voxel) covering the volume of interest. We used the following parameters : Time of Repetition TR=25ms, Time of Echo TE=3.1ms, flip Angle=20°, slice thickness=1.4 mm. Using open source software 3D Slicer (https://www.slicer.org/) 3D patient-specific models obtained from gathering images of the angiographic sequences. After gathering the images, we truncate the (ICA) arteries to obtain four geometrical models (Figure 1- (1-4)).

B. Blood flow simulation :

Inside the geometry, the blood flow behaviour can be described by unsteady Navies Stokes equations given by equations (1) and (2) [21]:

$$\nabla . v = 0 \qquad (1)$$

$$\rho \frac{\partial u}{\partial t} + \rho u . \nabla u - \nabla \sigma(u, p) = f \qquad (2)$$

In these equations, ρ is the density, p the pressure and v the velocity of the fluid.

For the blood flow simulations, we used finite elements method present in the solver of COMSOL Multiphysics Software. The flow was considered laminar and the blood is supposed incompressible, newtonian fluid with a density ρ=1060Kg/m^3 and a dynamic viscosity $\eta = 4mPa.s$[12, 17, 22]. During the simulation, the vascular wall was considered rigid with no-slip condition [23]. The solver tolerance was 10^{-3}, and time stepping tolerance was 10^{-2}; Due to the absence of patient-specific inlet flow rate waveform, we have been forced to use a non-specific-patient data to perform our study. For simulations, a pulsatile inlet volumic flow rate was applied. A pressure waveform was applied in outlet, we used three pulses (or cardiac cycles) as it shows in figure 2, where the first is used to examine solution convergence and the second to ensure that numerical stability was reached [22].
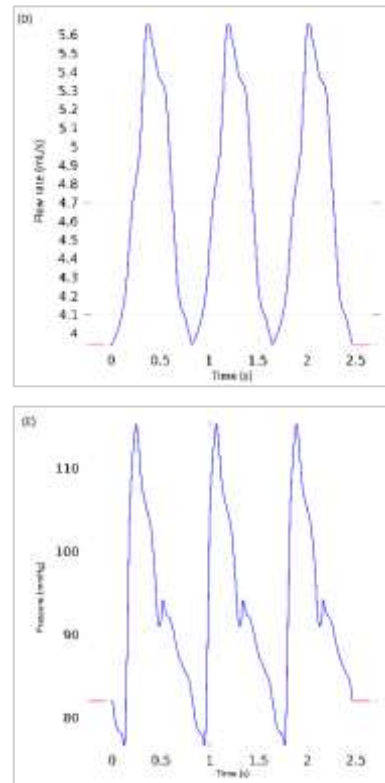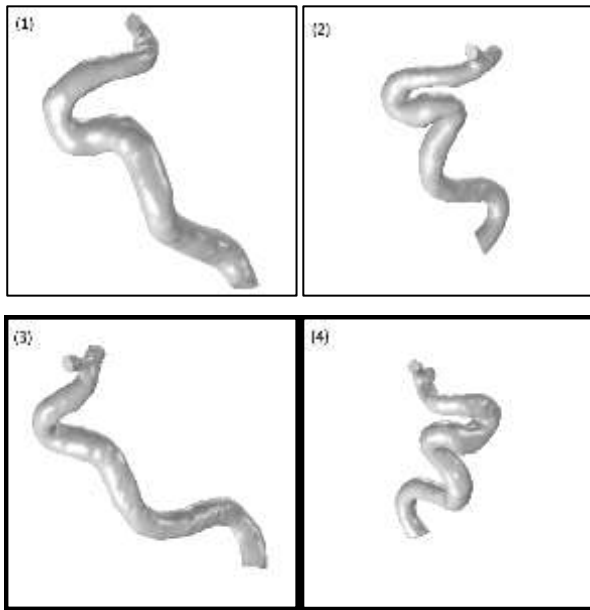
Figure 1: Four internal carotid artery (ICA) were analysed in this study (ICA (1), (2), (3) and (4))

(1) typical ICA of a 49-year-old female, (2) ICA of an old adult female, (3) ICA obtained from a 43-year-old male, and (4) ICA of a 73-year-old male.

(A-D) Inlet waveforms boundary conditions applied, (E) The pressure Waveform applied as outlet boundary condition.

In order to assess the effects of Inlet waveforms inside ICA geometrical model, four inlet waveforms were applied as inlet boundary conditions. The first (figure 1.A) was a waveform obtained from 17 healthy normal young volunteers [24], the second (figure 1.B) was a typical ICA waveform of a subject of 94 years old [25], the third waveform (figure 1.C) was an ICA waveform from a normal subject [23]. The fourth waveform (figure 1.D) was from female patient of 56 years old with an ICA aneurysm [26]. A pressure waveform (figure 1.E) was applied as outlet.

In this work, we appreciate the effect of the change of the inlet waveforms on pressure, WSS, TAWSS and velocity streamlines.

3. RESULTS:

Figure 2 shows the WSS distribution inside the different ICA using the four inlet waveforms. It is clearly showed that different waveforms produce the same WSS distribution at the systolic time. However, we can also see that the maximal values changes by changing the inlet waveform at the same ICA. In addition the obtained values have important changes between the four ICAs. Figure 3

29

shows a quantitative comparison of the maximal values of WSS (MWSS) obtained after CFD simulation; we can see that by changing the inlet waveforms boundaries

conditions, the MWSS at systolic times change : 20-25% for individual values and exceed twice the values between ICA-1- and the other ICAs.
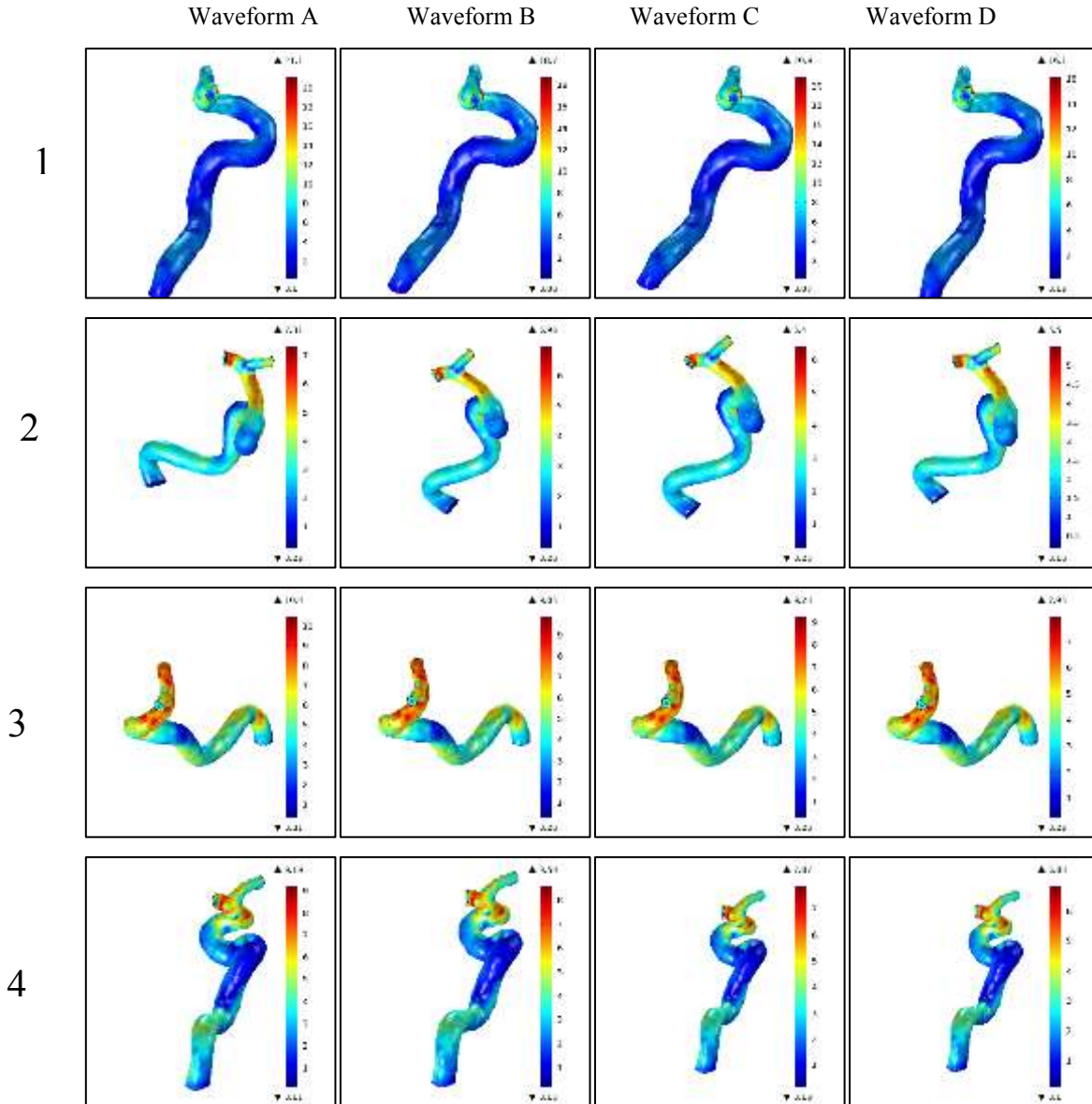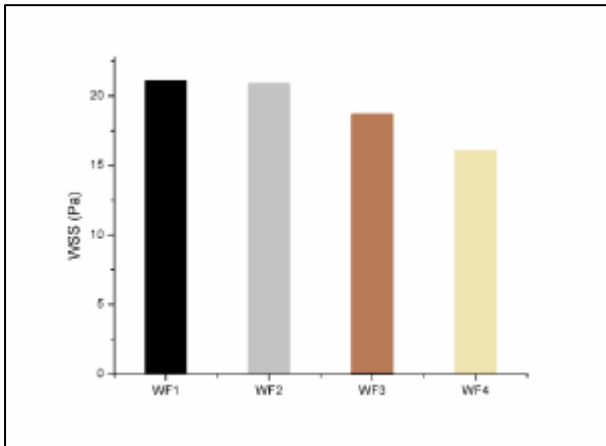
| Waveform A | Waveform B | Waveform C | Waveform D |

Figure 2. WSS distributions at the four ICAs (1), (2), (3) and (4) from pulsatile flow simulations using the four different waveforms (A), (B), (C) and (D) using the same mean inflow boundaries conditions.

Figure 4 shows the distributions of time-averaged WSS (TAWSS) predicted by the four pulsatile simulations with different applied inlet waveforms. For each ICA, different waveforms give almost identical TAWSS contour distributions in the segments of each ICA. However, we observed regional peak of TAWSS for the four ICA with the waveform (C).

Figure 5 shows the pressure repartition inside the four ICAs after simulation process using pulsatile inlet waveforms (1), (2), (3), and (4). We can see that there is a change in the pressure inside the ICAs between the different applied waveforms. For ICA-1- pressure varies in

the range of 84 to 122 mmHg for the minimum pressure and in the range of 99 to 141 mmHg for maximum values. ICA-2- pressure varies in the range of 78 to 112 mmHg for the minimum pressure and in the range of 93 to 133 mmHg for maximum values. ICA-3- pressure varies in the range of 83 to 122 mmHg for the minimum pressure and in the range of 100 to 142 mmHg for maximum values. ICA-4- pressure varies in the range o 123 to 169 mmHg for the minimum pressure and in the range of 132 to 182 mmHg for maximum values. The obtained values show that each waveforms applied act differently between individual and each ICA used in this work.
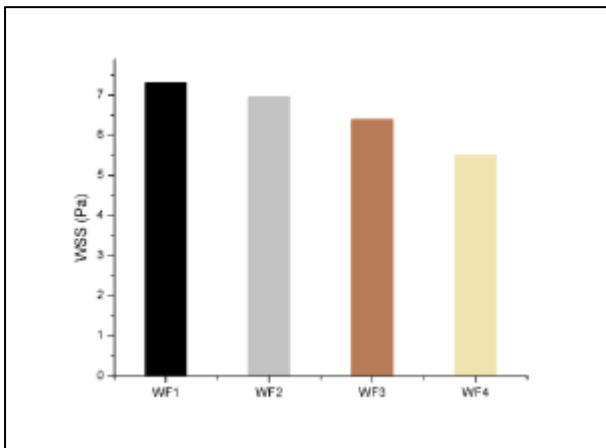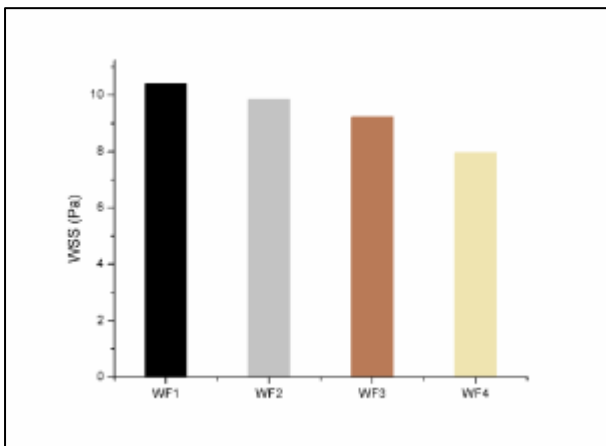
ICA –1-

ICA -4-
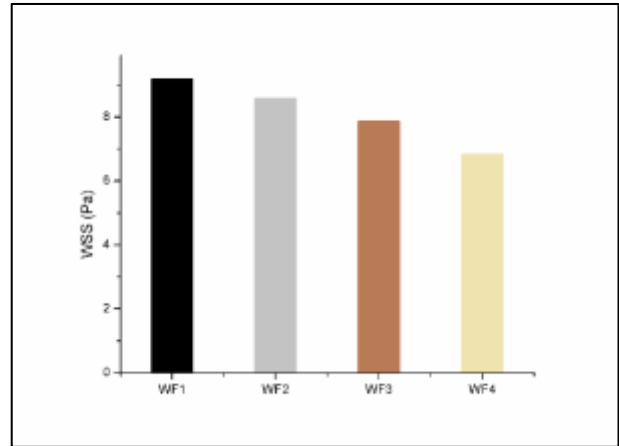
ICA -2-

Figure 3. Quantitative comparison of Maximum WSS (MWASS) for the different used waveforms.

Figure 6 shows the instantaneous velocity streamlines at the systolic time inside the ICAs using the fours waveforms with the same mean inflow applied as boundaries conditions to CFD. Velocity shows a regular flowing of the blood inside the vessel. However, figure shows that for each inlet waveform boundaries conditions applied, we find different values of velocity inside the ICA. Velocities found was ranged in 0.81m/s to 1.43 m/s with a maximum found in ICA-1- with waveforms (B) and (C) in where we located maximum value of WSS.
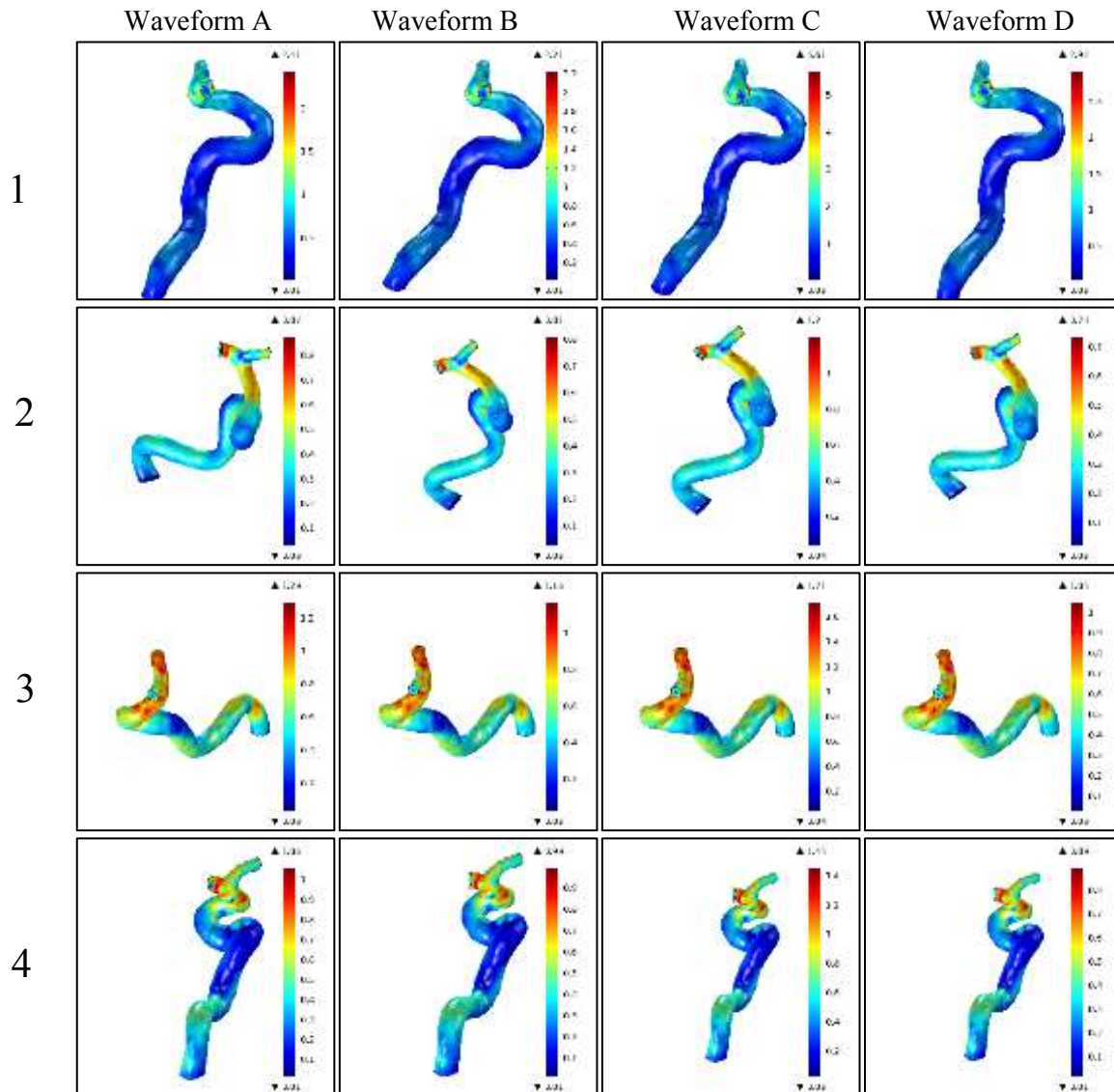
ICA –3-

Waveform A	Waveform B	Waveform C	Waveform D

Figure 4. TAWSS distribution after the application of the four inlet waveform boundaries conditions to the CFD.

4. *DISCUSSION:*

Since the introduction of image-based patient-specific computational fluid dynamics (CFD), this method has been widely used to investigate the role of thermodynamics in the development of cerebrovascular pathologies [15]. Image-based CFD requires assumptions like blood behaviour, artery wall dimensions, and inlet and/or outlet boundaries conditions [12, 13], in which depends the accuracy of CFD results.

Several studies demonstrated the accuracy of CFD to estimate hemodynamic factors inside realistic arteries in where a good quantitative agreement was observed between experimental and numerical velocities and WSS values using different modalities like PC-MRI [8, 27-30]

In the clinical routine, the patient specific flow measurements are not allowed, therefore CFD researchers employ non-patient specific flow waveforms as inlet boundaries conditions [31]. In this study, we assess the effects of the change of inlet waveform on hemodynamic inside normal cerebral arteries. We have examined these effects on four important hemodynamic parameters, which are WSS, pressure, TAWSS and velocity streamlines.
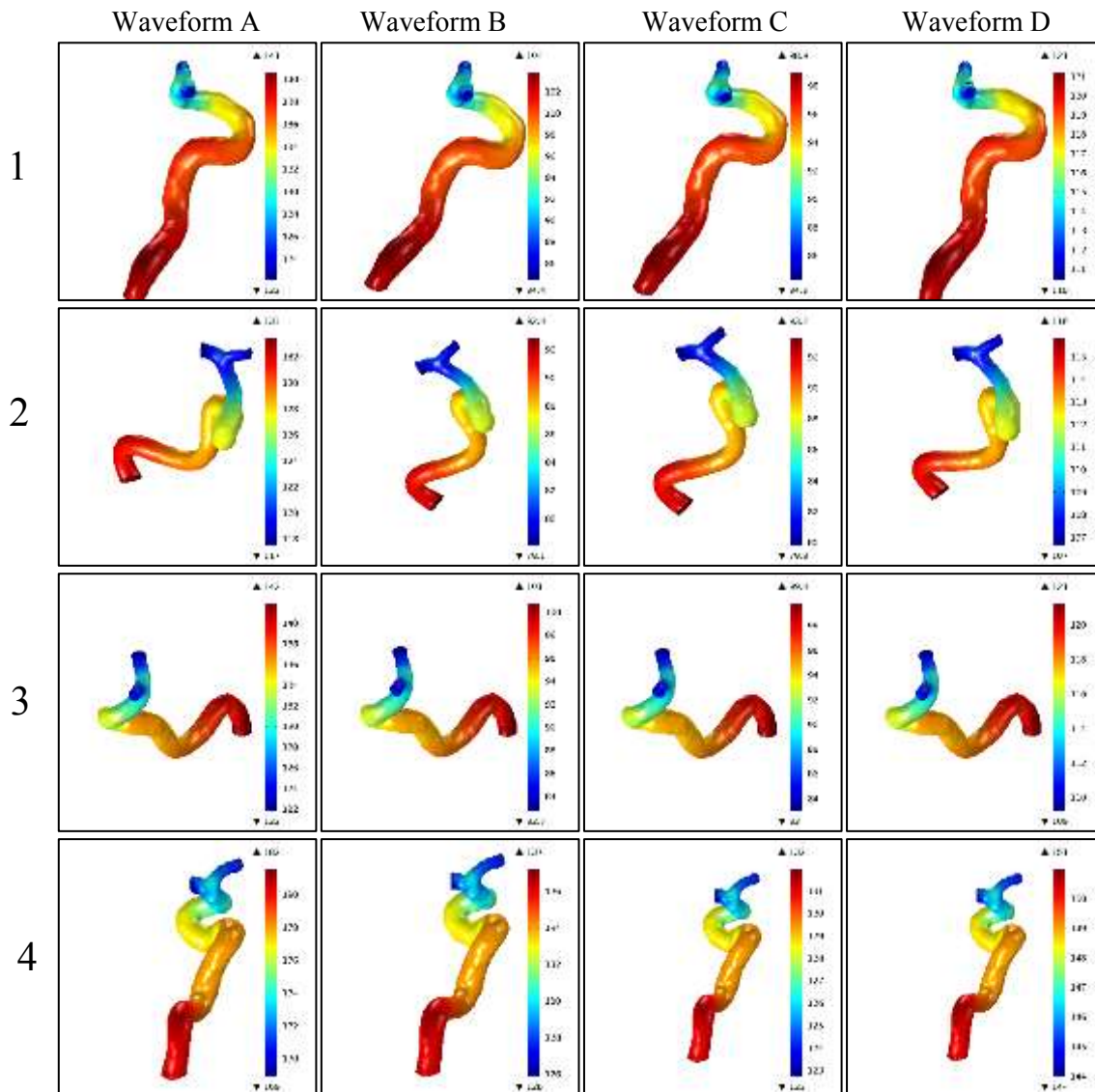
Figure 5. Pressure distribution inside the ICAs (1), (2), (3) and (4) after CFD simulation using the four-inlet waveforms boundary condition.

We found that WSS is highly influenced by the inlet waveform, which is due to the effects on the acceleration and deceleration of the flow. In addition, the pressure forces were highly influenced by the change of inlet waveform, this change is caused by the complex transitional flow dynamics effected by the inertial and viscous forces [31].

However, we found that TAWSS have small changes, which is in agreement with findings of [26] suggesting that CFD carried out under the same inlet flow rate for the same group of geometries in the same analysis methods, using different waveform boundaries conditions, could give similar time-averaged WSS distributions and magnitudes.
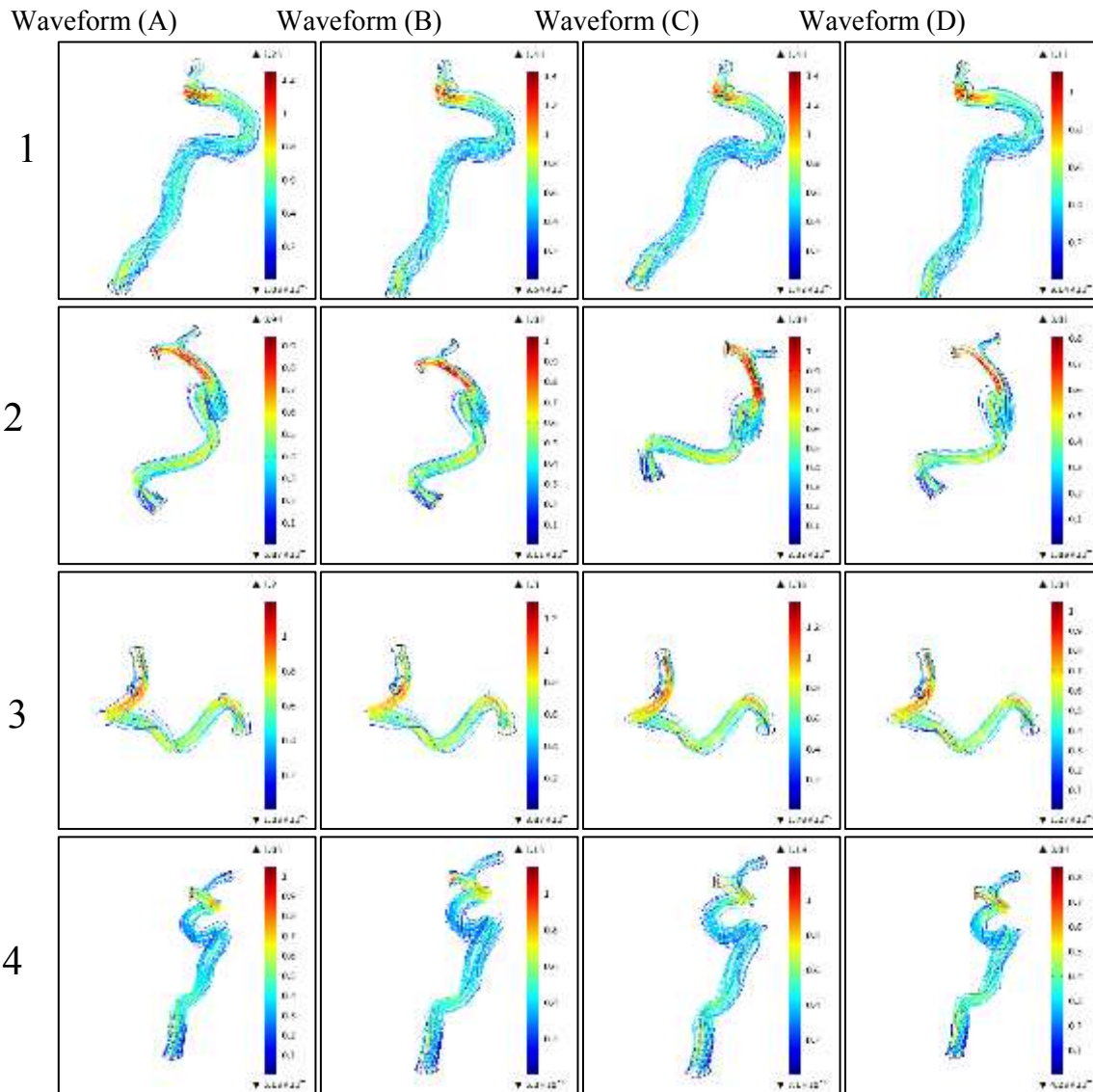
Waveform (A)	Waveform (B)	Waveform (C)	Waveform (D)

Figure 6. Velocity streamlines obtained after CFD using the different inlet waveform boundary condition applied.

Our findings demonstrate that the change in the inlet waveform may affect the hemodynamic parameter inside normal cerebral arteries, which supports the findings from few studies using CFD simulation. For example, several hemodynamic factors (WSS and Oscillatory Shear index (OSI)) were compared in [24] for two cases using patient specific waveforms and idealized averaged waveform from [32], as conclusion, they suggested that patient specific information flow may be necessary [33].

In another research, a comparison between flow velocities extracted from PC-MRI and flow velocities obtained using intra-arterial doppler angiography reveals differences in flow velocities which is consistent with our findings [34]

In this work, we can report several limitations like assumptions about the blood newtonian nature and rigid walls commonly adopted in a CFD model, which are believed to effect the flow field (for example

overestimation of WSS values) [35]. However, we believe that the effects of these boundaries conditions are minimal. In addition, the number of ICA studied which is limited. The aim of our work is to demonstrate the importance of patient-specific inflow when using surrogate waveform in a CFD study. However, more investigations must be done to validate our finding.

CONCLUSION

In this paper, we performed a patient specific CFD to investigate the effects of the change of inlet waveform on the hemodynamic inside healthy ICA. Inlet waveform has an important impact on the instantaneous hemodynamic parameters, however the time-averaged parameters remains constant.

Patient specific waveform is required for the accuracy of patient specific hemodynamics to investigate potential cerebrovascular pathologies.

REFERENCES

[1] R. J. Traystman, "Chapter 1 - Cerebrovascular Anatomy and Hemodynamics A2 - Caplan, Louis R," in *Primer on Cerebrovascular Diseases (Second Edition)*, J. Biller, M. C. Leary, E. H. Lo, A. J. Thomas, M. Yenari, and J. H. Zhang, Eds., ed San Diego: Academic Press, 2017, pp. 5-12.

[2] N. Westerhof, N. Stergiopulos, and M. I. Noble, *Snapshots of hemodynamics: an aid for clinical research and graduate education*: Springer Science & Business Media, 2010.

[3] D. M. Sforza, C. M. Putman, and J. R. Cebral, "Hemodynamics of cerebral aneurysms," *Annual review of fluid mechanics,* vol. 41, pp. 91-107, 2009.

[4] M. J. Cipolla, "The cerebral circulation," *Integrated systems physiology: From molecule to function,* vol. 1, pp. 1-59, 2009.

[5] A. M. Malek, S. L. Alper, and S. Izumo, "Hemodynamic shear stress and its role in atherosclerosis," *Jama,* vol. 282, pp. 2035-2042, 1999.

[6] J. Ando and K. Yamamoto, "Effects of shear stress and stretch on endothelial function," *Antioxidants & redox signaling,* vol. 15, pp. 1389-1403, 2011.

[7] A. S. Turjman, F. Turjman, and E. R. Edelman, "Role of fluid dynamics and inflammation in intracranial aneurysm formation," *Circulation,* vol. 129, pp. 373-382, 2014.

[8] M. Cibis, W. V. Potters, F. J. Gijsen, H. Marquering, E. VanBavel, A. F. Steen, A. J. Nederveen, and J. J. Wentzel, "Wall shear stress calculations based on 3D cine phase contrast MRI and computational fluid dynamics: a comparison study in healthy carotid arteries," *NMR in Biomedicine,* vol. 27, pp. 826-834, 2014.

[9] J. R. Cebral, A. Radaelli, A. Frangi, and C. M. Putman, "Hemodynamics before and after bleb formation in cerebral aneurysms," in *Medical Imaging*, 2007, pp. 65112C-65112C-9.

[10] M. S. Alnæs, J. Isaksen, K.-A. Mardal, B. Romner, M. K. Morgan, and T. Ingebrigtsen, "Computation of hemodynamics in the circle of Willis," *Stroke,* vol. 38, pp. 2500-2505, 2007.

[11] V. C. Rispoli, J. F. Nielsen, K. S. Nayak, and J. L. Carvalho, "Computational fluid dynamics simulations of blood flow regularized by 3D phase contrast MRI," *Biomedical engineering online,* vol. 14, p. 110, 2015.

[12] Y. Hua, J. H. Oh, and Y. B. Kim, "Influence of Parent Artery Segmentation and Boundary Conditions on Hemodynamic Characteristics of Intracranial Aneurysms," *Yonsei medical journal,* vol. 56, pp. 1328-1337, 2015.

[13] A. Sarrami-Foroushani, M. N. Esfahany, H. S. Rad, K. Firouznia, M. Shakiba, and H. Ghanaati, "Effects of variations of flow and heart rate on intra-aneurysmal hemodynamics in a ruptured internal carotid artery aneurysm during exercise," *Iranian Journal of Radiology,* vol. 13, 2016.

[14] M. Viceconti, S. Olsen, L.-P. Nolte, and K. Burton, "Extracting clinically relevant data from finite element simulations," *Clinical Biomechanics,* vol. 20, pp. 451-454, 2005.

[15] M. A. Castro, M. C. A. Olivares, C. M. Putman, and J. R. Cebral, "Unsteady wall shear stress analysis from image-based computational fluid dynamic aneurysm models under Newtonian and Casson rheological models," *Medical & biological engineering & computing,* vol. 52, pp. 827-839, 2014.

[16] J. R. Cebral, C. M. Putman, M. T. Alley, T. Hope, R. Bammer, and F. Calamante, "Hemodynamics in normal cerebral arteries: qualitative comparison of 4D phase-contrast magnetic resonance and image-based computational fluid dynamics," *Journal of engineering mathematics,* vol. 64, pp. 367-378, 2009.

[17] D. Sekhane and K. Mansour, "Image-based Computational fluid dynamics (CFD) Modeling cerebral blood flow in the Circle of Willis," *Journal of Advanced Research in Physics,* vol. 6, 2016.

[18] I. D. Šutalo, A. V. Bui, S. Ahmed, K. Liffman, and R. Manasseh, "Modeling of flow through the circle of Willis and cerebral vasculature to assess the effects of changes in the peripheral small cerebral vasculature on the inflows," *Engineering Applications of Computational Fluid Mechanics,* vol. 8, pp. 609-622, 2014.

[19] D. Ivanov, A. Dol, O. Pavlova, and A. Aristambekova, "Modeling of human circle of Willis with and without aneurisms," *Acta of Bioengineering and Biomechanics,* vol. 16, pp. 121--129, 2014.

[20] Y. Ren, G.-Z. Chen, Z. Liu, Y. Cai, G.-M. Lu, and Z.-Y. Li, "Reproducibility of image-based computational models of intracranial aneurysm: a comparison between 3D rotational angiography, CT angiography and MR angiography," *Biomedical engineering online,* vol. 15, p. 50, 2016.

[21] D. Forti and L. Dedè, "Semi-implicit BDF time discretization of the Navier–Stokes equations

with VMS-LES modeling in a High Performance Computing framework," *Computers & Fluids,* vol. 117, pp. 168-182, 2015.

[22] L. Jing, J. Fan, Y. Wang, H. Li, S. Wang, X. Yang, and Y. Zhang, "Morphologic and hemodynamic analysis in the patients with multiple intracranial aneurysms: ruptured versus unruptured," *PloS one,* vol. 10, p. e0132494, 2015.

[23] J. R. Cebral, M. Hernández, and A. F. Frangi, "Computational analysis of blood flow dynamics in cerebral aneurysms from CTA and 3D rotational angiography image data," in *International congress on computational bioengineering*, 2003, pp. 191-198.

[24] M. D. Ford, N. Alperin, S. H. Lee, D. W. Holdsworth, and D. A. Steinman, "Characterization of volumetric flow rate waveforms in the normal internal carotid and vertebral arteries," *Physiological measurement,* vol. 26, p. 477, 2005.

[25] Y. Hoi, B. A. Wasserman, E. G. Lakatta, and D. A. Steinman, "Carotid bifurcation hemodynamics in older adults: effect of measured versus assumed flow waveform," *Journal of biomechanical engineering,* vol. 132, p. 071006, 2010.

[26] J. Xiang, A. Siddiqui, and H. Meng, "The effect of inlet waveforms on computational hemodynamics of patient-specific intracranial aneurysms," *Journal of biomechanics,* vol. 47, pp. 3882-3890, 2014.

[27] P. M. McGah, M. R. Levitt, M. C. Barbour, R. P. Morton, J. D. Nerva, P. D. Mourad, B. V. Ghodke, D. K. Hallam, L. N. Sekhar, and L. J. Kim, "Accuracy of computational cerebral aneurysm hemodynamics using patient-specific endovascular measurements," *Annals of biomedical engineering,* vol. 42, pp. 503-514, 2014.

[28] J. Jiang, K. Johnson, K. Valen-Sendstad, K.-A. Mardal, O. Wieben, and C. Strother, "Flow characteristics in a canine aneurysm model: a comparison of 4D accelerated phase-contrast MR measurements and computational fluid dynamics simulations," *Medical physics,* vol. 38, pp. 6300-6312, 2011.

[29] F. P. Salvucci, C. A. Perazzo, J. G. Barra, and R. L. Armentano, "Assessment of pulsatile wall shear stress in compliant arteries: Numerical model, validation and experimental data," in *Engineering in Medicine and Biology Society, 2009. EMBC 2009. Annual International Conference of the IEEE*, 2009, pp. 2847-2850.

[30] B. B. Lieber and C. Sadasivan, "Endoluminal scaffolds for vascular reconstruction and exclusion of aneurysms from the cerebral circulation," *Stroke,* vol. 41, pp. S21-S25, 2010.

[31] A. Geers, I. Larrabide, H. Morales, and A. Frangi, "Approximating hemodynamics of cerebral aneurysms with steady flow simulations," *Journal of biomechanics,* vol. 47, pp. 178-185, 2014.

[32] C. Karmonik, C. Yen, O. Diaz, R. Klucznik, R. G. Grossman, and G. Benndorf, "Temporal variations of wall shear stress parameters in intracranial aneurysms—importance of patient-specific inflow waveforms for CFD calculations," *Acta neurochirurgica,* vol. 152, pp. 1391-1398, 2010.

[33] B. Chung and J. R. Cebral, "CFD for evaluation and treatment planning of aneurysms: review of proposed clinical uses and their challenges," *Annals of biomedical engineering,* vol. 43, pp. 122-138, 2015.

[34] J. Schneiders, S. Ferns, P. van Ooij, M. Siebes, A. Nederveen, R. van den Berg, J. van Lieshout, G. Jansen, and C. Majoie, "Comparison of phase-contrast MR imaging and endovascular sonography for intracranial blood flow velocity measurements," *American Journal of Neuroradiology,* vol. 33, pp. 1786-1790, 2012.

[35] J. Xiang, M. Tremmel, J. Kolega, E. I. Levy, S. K. Natarajan, and H. Meng, "Newtonian viscosity model could overestimate wall shear stress in intracranial aneurysm domes and underestimate rupture risk," *Journal of neurointerventional surgery,* pp. neurintsurg-2011-010089, 2011.